# Multipole amplitudes of pion photoproduction on nucleons up to 2 GeV using dispersion relations and the unitary isobar model

I. G. Aznauryan*

*Yerevan Physics Institute, Alikhanian Brothers St.2, Yerevan 375036, Armenia*
(Received 8 August 2002; published 30 January 2003)

Two approaches for the analysis of pion photoproduction and electroproduction on nucleons in the resonance energy region are checked at $Q^2=0$ using the results of the GWU(VPI) partial-wave analysis of photoproduction data. The approaches are based on dispersion relations and the unitary isobar model. Within dispersion relations a good description of photoproduction multipoles is obtained up to $W=1.8$ GeV. Within the unitary isobar model, modified with increasing energy by the incorporation of Regge poles and with a unified Breit-Wigner parametrization of resonance contributions, a good description of photoproduction multipoles is obtained up to $W=2$ GeV.

## I. INTRODUCTION

It is known that dispersion relations (DR), and the unitary isobar model (UIM), constructed on the basis of an effective Lagrangian approach in Ref. [1], are widely used for the analysis of pion photoproduction and electroproduction data and for the extraction from these data of information on $\gamma^*N \to N^*$ vertices. In this paper our goal is to check these approaches at $Q^2=0$ using the results of a GWU(VPI) partial-wave analysis of pion photoproduction made from threshold to $W=2$ GeV (Refs. [2,3], and the SAID program). In the case of dispersion relations the main goal is to find the energy region of applicability of DR, since with increasing energy the utilization of DR is connected with the following problems: (a) at large angles the important $P_{33}(1232)$ resonance contribution requires, in the integrands of DR extrapolation to very large $x=\cos\theta$, and becomes arbitrary; (b) the unknown contribution of resonances with large masses ($M > 2$ GeV) can become important; and (c) the contribution of the Regge region ($W>2.5$ GeV) can also become important. From the results of this paper it follows that the role of these effects is insignificant up to $W=1.8$ GeV, and DR can be reliably used in this energy region.

In the case of the UIM our goal is to find an adequate description of the resonance and background contributions in order to extend this model to $W=2$ GeV. It is known that the background of the UIM which consists of the minimal number of diagrams (the nucleon exchanges in the $s$ and $u$ channels and the $t$ channel $\pi$, $\rho$, and $\omega$ exchanges) is motivated only at threshold (Refs. [4,5]) and in the first resonance region (Refs. [1,6], and references therein). As will be argued in Sec. III, the extension of this background above the first resonance region cannot be satisfactory. Moreover, continued to 2 GeV and higher, the background of Ref. [1] strongly contradicts experimental data. We will modify the UIM in such a way that with increasing energy the amplitudes of the model will transform into the amplitudes in the Regge pole

regime which starts practically at $W=2.5$ GeV. We will demonstrate that incorporation of Regge poles into the background with increasing energy results in a good description of the GWU(VPI) photoproduction multiple amplitudes in the resonance energy region up to $W=2$ GeV. This description will be obtained using a standard Breit-Wigner parametrization for the resonance contributions, as suggested in Ref. [7]. Only for the multipoles $M_{1+}^{3/2}$ and $E_{1+}^{3/2}$, corresponding to the $P_{33}(1232)$ resonance, will a slight modification be made in order to satisfy the Watson theorem [8]. Let us note that in order to reproduce photoproduction multiple amplitudes in the UIM of Ref. [1], a complicated parametrization of resonance contributions has been used. Such a complication is caused by the fact that above the first resonance region background contributions into some multiple amplitudes in Ref. [1] become too large, and in order to compensate them resonance contributions have been strongly deformed.

In Sec. II we will present our results obtained within dispersion relations. First, in Sec. II A we will present the results for multipole amplitudes $M_{1+}^{3/2}$ and $E_{1+}^{3/2}$ which correspond to the $P_{33}(1232)$ resonance. It will be shown, that DR for $M_{1+}^{3/2}$ and $E_{1+}^{3/2}$ can be transformed into singular integral equations. These multipoles will be found via solutions of these equations. Further, in Sec. II B, imaginary parts of the contributions corresponding to other resonances will be found using the results of the GWU(VPI) analysis and assuming a Breit-Wigner parametrization for resonance contributions. We will also find nonresonance contributions to imaginary parts of $E_{0+}^{(0,1/2,3/2)}$, $M_{1-}^{(3/2)}$, $M_{1+}^{(0,1/2)}$ and $E_{1+}^{(0,1/2)}$ which are not small at small energies due to large $\pi N$ phases $\delta_{0+}^{1/2,3/2}$, $\delta_{1-}^{3/2}$, and $\delta_{1+}^{1/2}$. These contributions will be found using DR and the Watson theorem. Finally, in Sec. II C, using DR, real parts of the multipole amplitudes will be found. In this section the contribution of the multipole $M_{1+}^{(3/2)}$, coresponding to the $P_{33}(1232)$ resonance into DR for other multipoles, will be investigated, and it will be shown that at $W>1.8$ GeV there is significant arbitrariness in the real parts of some multipole amplitudes connected with this contribution. The dispersion integrals over the high energy region will be also estimated in Sec. II C, and it will

*Email addresses: aznaury@jlab.org,
aznaur@jerewan1.yerphi.am

be shown that the role of these integrals in the resonance energy region is insignificant.

In Sec. III we will discuss and present the modified UIM and will present the results obtained within this model. Conclusions will be made in Sec. IV.

## II. DISPERSION RELATIONS

We use fixed-$t$ dispersion relations for invariant amplitudes. We derive real parts of multipole amplitudes via an expansion of results obtained over multipoles. The invariant amplitudes are chosen following Ref. [9] in accordance with the definition of the hadron electromagnetic current,

$$
I^\mu = \bar{u}(p_2)\gamma_5 \left\{ \frac{B_1}{2} [\gamma^\mu(\gamma\tilde{k}) - (\gamma\tilde{k})\gamma^\mu] + 2P^\mu B_2 + 2\tilde{q}^\mu B_3 \right.
$$
$$
+ 2\tilde{k}^\mu B_4 - \gamma^\mu B_5 + (\gamma\tilde{k})P^\mu B_6 + (\gamma\tilde{k})\tilde{k}^\mu B_7
$$
$$
\left. + (\gamma\tilde{k})\tilde{q}^\mu B_8 \right\} u(p_1), \tag{1}
$$

where $\tilde{k}$, $\tilde{q}$, $p_1$, and $p_2$ are four-momenta of the virtual photon, pion, initial and final nucleons, respectively, $P = \frac{1}{2}(p_1 + p_2)$, and $B_1, B_2, \ldots, B_8$ are invariant amplitudes which are functions of the invariant variables $s = (\tilde{k} + p_1)^2$, $t = (\tilde{k} - \tilde{q})^2$, and $Q^2 \equiv -\tilde{k}^2$.

The conservation of the hadron electromagnetic current leads to the relations

$$
4Q^2 B_4 = (s-u)B_2 - 2(t+Q^2-m_\pi^2)B_3,
$$
$$
2Q^2 B_7 = -2B_5' - (t+Q^2-m_\pi^2)B_8, \tag{2}
$$

where $B_5' \equiv B_5 - \frac{1}{4}(s-u)B_6$. So only six of the eight invariant amplitudes are independent. As independent amplitudes let us choose $B_1, B_2, B_3, B_5', B_6$, and $B_8$. The relations between these amplitudes and the multipoles are given in Appendix A. For all amplitudes $B_1^{(\pm,0)}, B_2^{(\pm,0)}, B_3^{(+,0)}$, $B_5'^{(\pm,0)}, B_6^{(\pm,0)}$, and $B_8^{(\pm,0)}$, except $B_3^{(-)}$, unsubtracted dispersion relations at fixed $t$ can be written

$$
ReB_i^{(\pm,0)}(s,t,Q^2) = R_i^{(v,s)}(Q^2)\left(\frac{1}{s-m_N^2} + \frac{\eta_i\eta^{(+,-,0)}}{u-m_N^2}\right)
$$
$$
+ \frac{P}{\pi}\int_{s_{thr}}^\infty Im\ B_i^{(\pm,0)}(s',t,Q^2)
$$
$$
\times \left(\frac{1}{s'-s} + \frac{\eta_i\eta^{(+,-,0)}}{s'-u}\right)ds', \tag{3}
$$

where $R_i^{(v,s)}(Q^2)$ are residues in the nucleon poles (they are given in Appendix B), $\eta_1 = \eta_2 = \eta_6 = 1$, $\eta_3 = \eta_5' = \eta_8 = -1$, $\eta^{(+)} = \eta^{(0)} = 1$, $\eta^{(-)} = -1$, and $s_{thr} = (m_N + m_\pi)^2$. For the amplitude $B_3^{(-)}$ we take the subtraction point at infinity. In this case, using current conservation conditions (2), we have

$$
ReB_3^{(-)}(s,t,Q^2) = R_3^{(v)}(Q^2)\left(\frac{1}{s-m_N^2} + \frac{1}{u-m_N^2}\right)
$$
$$
- \frac{eg}{4\pi}\frac{F_\pi(Q^2)}{t-m_\pi^2}
$$
$$
+ \frac{P}{\pi}\int_{s_{thr}}^\infty Im\ B_3^{(-)}(s',t,Q^2)\left(\frac{1}{s'-s}\right.
$$
$$
\left. + \frac{1}{s'-u} - \frac{4}{s'-u'}\right)ds', \tag{4}
$$

where the Born term, in addition to the nucleon poles, also includes pion exchange in the $t$ channel.

Amplitudes $B^{(+)}$ and $B^{(-)}$ correspond to isovector photons and are related to amplitudes with a definite total isospin in the $s$ channel by

$$
B^{(+)} = \frac{1}{3}(B^{(1/2)} + 2B^{(3/2)}), \quad B^{(-)} = \frac{1}{3}(B^{(1/2)} - B^{(3/2)}). \tag{5}
$$

Amplitude $B^{(0)}$ corresponds to the isoscalar photon.

Amplitudes corresponding to reactions with a definite charge states are

$$
B(\gamma + p \to p + \pi^0) = B^{(+)} + B^{(0)},
$$
$$
B(\gamma + n \to n + \pi^0) = B^{(+)} - B^{(0)}, \tag{6}
$$
$$
B(\gamma + p \to n + \pi^+) = 2^{1/2}(B^{(0)} + B^{(-)}),
$$
$$
B(\gamma + n \to p + \pi^-) = 2^{1/2}(B^{(0)} - B^{(-)}).
$$

We will use also the notations

$$
_pB^{\frac{1}{2}} = B^{(0)} + \frac{1}{3}B^{(1/2)}, \quad _nB^{\frac{1}{2}} = B^{(0)} - \frac{1}{3}B^{(1/2)}, \tag{7}
$$

where the subscript $p(n)$ denotes a proton (neutron) target.

### A. $P_{33}(1232)$ resonance

Let us write dispersion relations for the multipole amplitudes $M_{1+}^{3/2}/kq$ and $E_{1+}^{3/2}/kq$ in the form

$$
M(W) = M^B(W) + \frac{1}{\pi}\int_{W_{thr}}^{W_{max}} \frac{ImM(W')}{W'-W-i\varepsilon}dW'
$$
$$
+ \frac{1}{\pi}\int_{W_{thr}}^{W_{max}} K(W,W')ImM(W')dW', \tag{8}
$$

where $M(W)$ denotes any of multipoles $M_{1+}^{3/2}/kq$, $E_{1+}^{3/2}/kq$, $k$, and $q$, are the photon and pion 3-momenta in the c.m.s., $M^B(W)$, is the contribution of the Born term into these multipoles, $K(W,W')$ is a nonsingular kernel arising from the $u$-channel contribution to the disper-
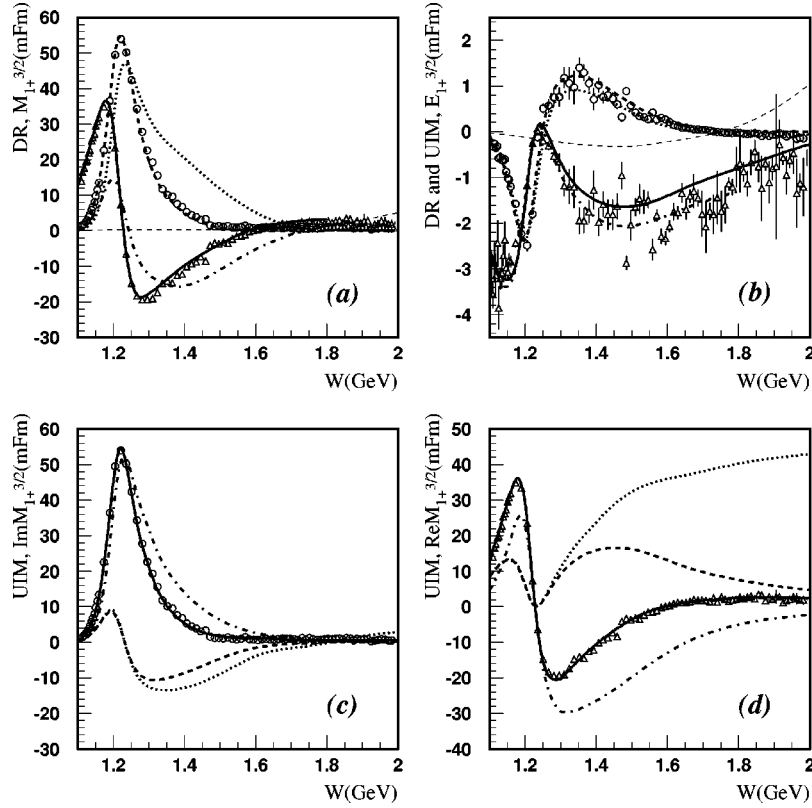
FIG. 1. (a) Multipole amplitude $M_{1+}^{3/2}$ within the DR. The results are obtained via a solution of the integral equation (8): solid and dashed curves correspond to the real and imaginary parts of the amplitude; dotted and dashed-dotted curves correspond to the contributions of homogeneous and particular solutions into $\mathrm{Im}M_{1+}^{3/2}$; and the thin dashed curve is the contribution of other multipoles into Eq. (8). (b) Multipole amplitude $E_{1+}^{3/2}$ within the DR and UIM. Dash-dotted and dashed curves are the real and imaginary parts of the amplitude obtained by the DR via solution of the integral equation (8); the thin dashed curve is the contribution of other multipoles into Eq. (8); and the solid and dotted curves are the real and imaginary parts of the amplitude obtained within the UIM with modified background [Eq (16)]. (c) $\mathrm{Im}M_{1+}^{3/2}$ in the UIM: the solid curve is the full result obtained with the modified background [Eq. (16)]; the dash-dotted and dashed curves correspond to the resonance and unitarized background contributions, respectively; and the dotted curve corresponds to the unitarized nonmodified background. (d) $\mathrm{Re}M_{1+}^{3/2}$ in the UIM: the legend is as for (c). In (a)–(d), the GWU(VPI) results from the SAID program are presented by open circles for the imaginary parts of the amplitudes, and by open triangles for those real parts. All amplitudes are in millifermi units.

sion integral and the nonsingular part of the $s$-channel contribution, $W_{max} = 1.8$ GeV. In relations (8) the following assumptions are made.

(a) For each of the amplitudes $M_{1+}^{3/2}/kq$ and $E_{1+}^{3/2}/kq$ we neglect the contributions of other multipoles into dispersion integrals. By our estimations they are small and do not affect our final results. These contributions are shown by thin dashed curves in Figs. 1(a) and 1(b). It is seen that up to 1.8 GeV they are practically equal to zero for $M_{1+}^{3/2}$ and are very small for $E_{1+}^{3/2}$.

(b) We neglect the integrals over $(W_{max} = 1.8$ GeV, $\infty)$. In Figs. 1(a) and 1(b) we present the results of the GWU(VPI) partial-wave analysis for $M_{1+}^{3/2}$ and $E_{1+}^{3/2}$ up to $W = 2$ GeV. It is seen that at 1.8 GeV$<W$ $<2$ GeV, $\mathrm{Im}M_{1+}^{3/2}$ and $\mathrm{Im}E_{1+}^{3/2}$ are practically equal to 0. The integrals over $(2$ GeV, $\infty)$ were estimated using the results of the Regge-pole analysis of high energy data made in Ref. [10]. These integrals turned out to be negligibly small.

Let us make one more assumption.

(c) We will use the Watson theorem from threshold to $W = 1.8$ GeV, assuming that $\delta_{1+}^{3/2}(W) \to \pi$, i.e., $\mathrm{Im}M(W)$

$\to 0$, when $W \to W_{max}$. From the results of the GWU(VPI) partial-wave analysis, presented in Figs. 1(a) and 1(b), it is seen that this is a reasonable assumption, taking into account that the $\pi N$ amplitude $h_{1+}^{3/2}(W)$ is elastic up to $W = 1.45$ GeV, and at $W = 1.45$ GeV, $\delta_{1+}^{3/2} = 157°$ [11]. So, in all integration regions we will take $\mathrm{Im}M(W) = h^*(W)M(W)$.

With these assumptions the dispersion relations for $M_{1+}^{3/2}$ and $E_{1+}^{3/2}$ turn into singular integral equations (8), which at $K(W,W') = 0$ have solutions in an analytical form [12,13],

$$M_{K=0}(W) = M_{part,K=0}^{B}(W) + c_{M}M_{K=0}^{hom}(W), \qquad (9)$$

where $M_{part,K=0}^{B}(W)$ is the particular solutions of Eq. (8) generated by $M^{B}$,

$$M_{part,K=0}^{B}(W) = M^{B}(W) + \frac{1}{\pi}\frac{1}{D(W)}$$

$$\times \int_{W_{thr}}^{W_{max}} \frac{D(W')h(W')M^{B}(W')}{W'-W-i\varepsilon}dW',$$

$$(10)$$

and

$$M^{hom}_{K=0}(W) = \frac{1}{D(W)} = \frac{W_{max}}{|W_{max} - W|}$$

$$\times \exp\left[\frac{W}{\pi}\int_{W_{thr}}^{W_{max}}\frac{\delta(W')}{W'(W'-W-i\varepsilon)}dW'\right] \quad (11)$$

is the solution of homogeneous equation (8) with $M^B = 0$. It

$$\sin^2\delta^{3/2}_{1+} = \frac{(4.27q^3)^2}{(4.27q^3)^2 + (q_r^2 - q^2)^2[1 + 40q^2(q^2 - q_r^2) + 21.4q^2]^2}, \quad (12)$$

which is a slightly modified version of the corresponding formula from Ref. [15], $q_r$ is the pion c.m.s. momentum at $W = M$. At 1.35 GeV$< W <$1.8 GeV, the phase was taken in the form

$$\delta = \pi - [\pi - \delta(W=1.35 \text{ GeV})]\left(\frac{q-q_2}{q_1-q_2}\right)^2, \quad (13)$$

where $q_1$ and $q_2$ are the pion c.m.s. momenta, respectively, at $W = 1.35$ and $W = 1.8$ GeV. Equations (12) and (13) reproduce with good accuracy the results of the GWU(VPI) analysis for $\delta^{3/2}_{1+}(W)$ from threshold to $W = 1.5$ GeV.

Our final results for $M^{3/2}_{1+}$ and $E^{3/2}_{1+}$, obtained by formulas (9)–(13) via adjusting the only unknown parameters $c_M$ and $c_E$, are presented in Figs. 1(a) and 1(b). It is seen that there is good agreement with the GWU(VPI) results. In Fig. 1(a) we also separately presented contributions of particular and homogeneous solutions into the imaginary part of $M^{3/2}_{1+}$.

### B. Imaginary parts of multipole amplitudes up to 2 GeV

In the energy region below $W = 2$ GeV the imaginary parts of multipole amplitudes are determined mainly by resonance contributions. These contributions for resonances which are seen in the GWU(VPI) analysis at $W < 2$ GeV [except $P_{33}(1232)$] were parametrized using the Breit-Wigner form given in Appendix C. A good description of the imaginary parts of multipole amplitudes was obtained with the Breit-Wigner parameters presented in Table I.

At small energies imaginary parts of the amplitudes $E^{(0,1/2,3/2)}_{0+}$, $M^{(3/2)}_{1-}$, $M^{(0,1/2)}_{1+}$, and $E^{(0,1/2)}_{1+}$ also contain noticeable nonresonance contributions due to large $\pi N$ phases $\delta^{1/2,3/2}_{0+}$ and $\delta^{3/2}_{1-}$ $\delta^{1/2}_{1+}$. Up to $W = 1.3$ GeV these contributions were found using DR and the Watson theorem. At higher energies they were reduced to 0. Our final results for the imaginary parts of the multipole amplitudes obtained in the way described in this section are presented by dashed curves in Fig. 2.

enters solution (9) with an arbitrary weight, i.e., multiplied by an arbitrary constant $c_M$.

At $K(W,W') \neq 0$ one can transform singular integral equation (8) into a nonsingular integral equation [14]. The solution of this equation turned out to be very close to Eq. (9).

From Eqs. (9)–(11) it is seen that with a given $M^B(W)$, the particular and homogeneous solutions of integral equation (8) are determined only by the phase $\delta^{3/2}_{1+}(W)$. In our calculations, at $W < 1.35$ GeV, this phase was taken in the form

### C. Real parts of multipole amplitudes

Real parts of multipole amplitudes were found using dispersion relations (3) and (4). Let us present dispersion integrals in these relations in the form

$$\int_{W_{thr}}^{\infty} = \int_{W_{thr}}^{2 \text{ GeV}} + \int_{2 \text{ GeV}}^{2.5 \text{ GeV}} + \int_{2.5 \text{ GeV}}^{\infty}. \quad (14)$$

Imaginary parts of the amplitudes in the integrals over the resonance energy region from threshold to 2 GeV were found via expansion of invariant amplitudes in the integrands over multipole amplitudes using relations inverse to Eq. (A1), relations (A3) and the imaginary parts of the multipole amplitudes obtained in Secs. II A and II B. As we use DR at a fixed $t$, the argument in the Legendre polynomials in these

TABLE I. Parameters in the Breit-Wigner formula from Appendix C, found via a description of imaginary parts of the multipole amplitudes. In the parentheses the parameters found within the UIM are presented in the cases when they differ from the parameters found in this section.

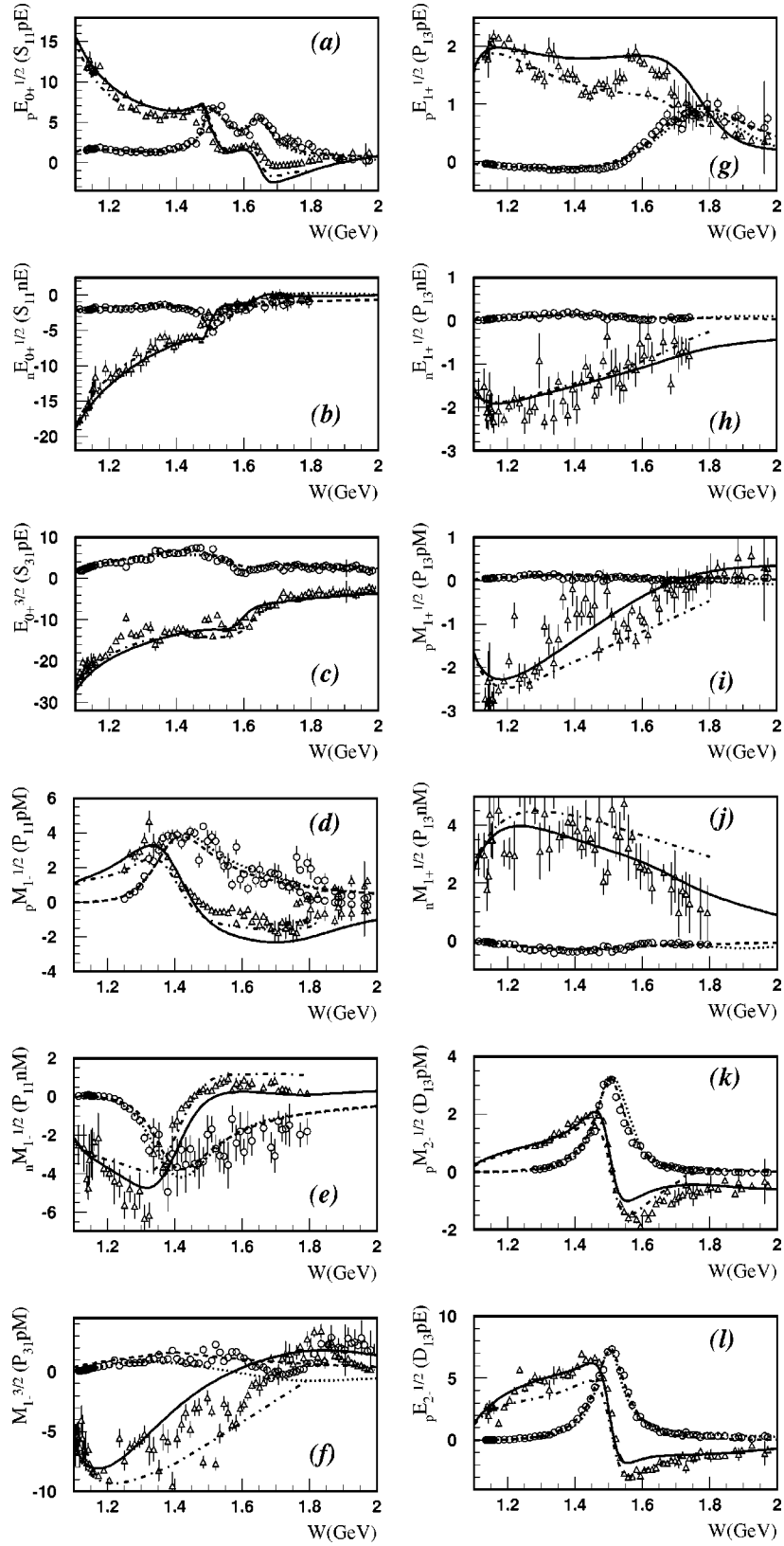| Resonance | $M$, GeV | $\Gamma$, GeV | $X$ |
|---|---|---|---|
| $P_{11}(1440)$ | 1.45(1.46) | 0.3 | 0.3 |
| $S_{11}(1535)$ | 1.52 | 0.11(0.12) | 0.5 |
| $D_{13}(1520)$ | 1.51 | 0.12(0.1) | 0.1(0.3) |
| $S_{11}(1650)$ | 1.65 | 0.08(0.11) | 0.5 |
| $F_{15}(1680)$ | 1.68 | 0.13 | 0.2(0.5) |
| $P_{13}(1720)$ | 1.8 | 0.38(0.35) | 0.5(0.4) |
| $S_{31}(1620)$ | 1.61(1.62) | 0.14 | 0.5 |
| $D_{33}(1700)$ | 1.65 | 0.25 | 0.22(0.2) |
| $F_{37}(1950)$ | 1.92(1.93) | 0.3 | 0.5 |

FIG. 2. Multipole amplitudes within the DR and UIM. Dash-dotted and dashed curves are the real and imaginary parts of amplitudes obtained by the DR. Solid and dotted curves are the real and imaginary parts of amplitudes obtained within a UIM with a modified background [Eq. (16)]. Plotted are the multipole amplitudes in millifermi units. In parentheses the notations of multipole amplitudes in the SAID program are given. The GWU(VPI) results from the SAID program are presented by open circles for the real parts of the amplitudes, and by open triangles for those imaginary parts.
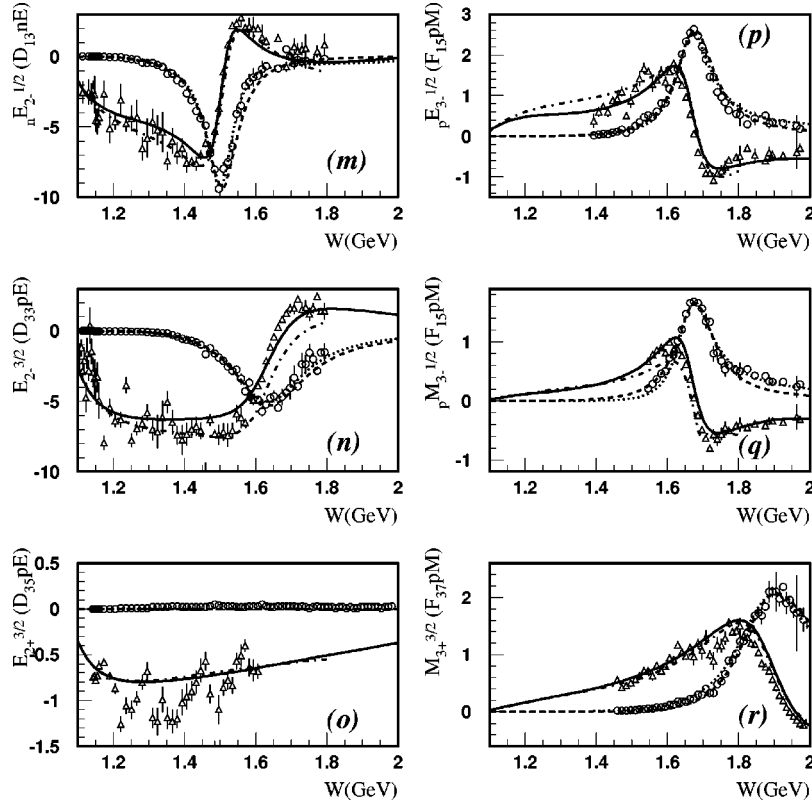
FIG. 2. (*Continued*).

expansions is equal to $\cos\theta' = (t + Q^2 - m_\pi^2 + 2k_0'q_0')/2|\mathbf{k}'||\mathbf{q}'|$, where $k'$ and $q'$ are the four-momenta of the virtual photon and pion corresponding to $s'$. When $s' < s$, we have $\cos\theta' > \cos\theta$, and in the dispersion integrals a problem can arise due to the possible divergence of the partial-wave expansion. This problem has been discussed in a number of papers (see, for example, Ref. [16] and references therein). However it remains unclear up to which $\cos\theta' > 1$ the partial-wave expansion [Eq. (A3)] can be used in the dispersion integrals. In Ref. [16] a good description of photoproduction data was obtained using fixed-$t$ dispersion relations at $|t| < 1.6$ GeV$^2$, i.e., for the full angular range up to $W = 1.78$ GeV. This permits an empirical conclusion that the partial-wave expansion [Eq. (A3)] can be used in the dispersion integrals up to $|t| = 1.6$ GeV$^2$. In this paper this conclusion is confirmed by the results of the comparison of the real parts of the photoproduction multipole amplitudes obtained by the fixed-$t$ dispersion relations with the results of the GWU(VPI) analysis.

Imaginary parts of the amplitudes in the integrals over the high energy region from 2.5 GeV to $\infty$ can be found using the results of Regge-pole analysis made in Ref. [10]. The method used to construct the amplitudes in Ref. [10] is described in Appendix D. This analysis is made in gauge-invariant form and using invariant amplitudes. For this reason its results can be easily used for the calculation of high energy integrals in dispersion relations (3) and (4). The role of these integrals turned out to be negligible in the real parts of multipoles in the I and II resonance regions and very small in the III and IV resonance regions. Imaginary parts of the

amplitudes in the integrals over the intermediate energy region were calculated via an interpolation of the imaginary parts of the amplitudes between the regions: $W < 2$ GeV and $W > 2.5$ GeV.

Our final results for real parts of the multipole amplitudes are presented in Fig. 2 by dash-dotted curves. Let us note that in Fig. (2) all amplitudes for which the GWU(VPI) analysis gives definite results are presented. It is seen that the agreement with the GWU(VPI) results is satisfactory up to $W = 1.8$ GeV. At higher energies in some multipoles, noticeable deviations from the GWU(VPI) analysis arise. Most probably they are connected with the above discussed divergence of the partial-wave expansions in the dispersion integrals. The main uncertainty which can arise due to this divergence is connected with the contribution of the multipole $M_{1+}^{3/2}$ corresponding to the $P_{33}(1232)$ resonance. The contribution of this multipole, which is large by itself, sharply grows with increasing energy. This is demonstrated in Figs. 1(b) and 3 for the amplitudes $E_{1+}^{3/2}$, $E_{0+}^{1/2,3/2}$, and $M_{1-}^{1/2,3/2}$. At $W > 1.7 - 1.8$ GeV these amplitudes are much smaller than the $P_{33}(1232)$ resonance contribution [see Figs. 2(a)–2(f)]; therefore, they should be obtained as differences of two large contributions, one of which, the $P_{33}(1232)$ contribution, contains arbitrariness. In addition, when we approach $W = 2$ GeV, the uncertainty connected with the unknown contributions of the resonances with $M > 2$ GeV can become significant. For these reasons multipole amplitudes obtained by DR at $W > 1.8$ GeV are not reliable, and we do not present them in Fig. 2.
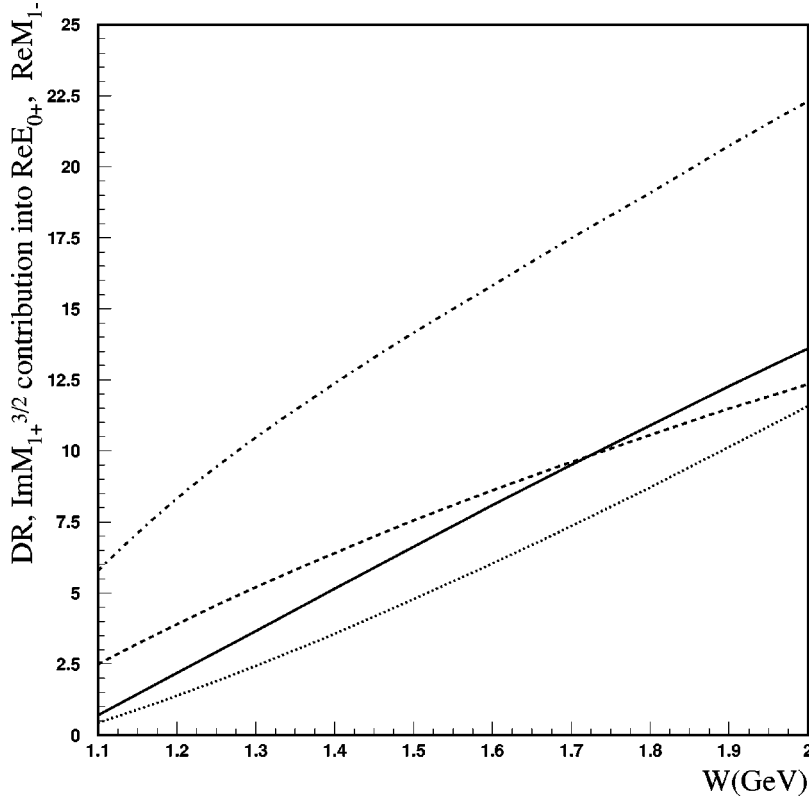
FIG. 3. The contributions of the integral over $M_{1+}^{3/2}$ (in millifermi units) into the real parts of the multipole amplitudes $E_{0+}^{1/2}$ (dashed curve), $E_{0+}^{3/2}$ (dashed-dotted curve), $M_{1-}^{1/2}$ (solid curve), and $M_{1-}^{3/2}$ (dotted curve) within dispersion relations.

## III. UNITARY ISOBAR MODEL

The unitary isobar model is based on the effective Lagrangian approach which was introduced in Refs. [4,5] to reproduce low energy results of current algebra and PCAC. Within the approach of Refs. [4,5] the pion photoproduction amplitudes consist of nucleon exchanges in the $s$ and $u$ channels, and the $t$ channel $\pi$ exchange with a pseudovector $\pi NN$ coupling. These contributions describe well pion photoproduction at threshold (Ref. [5]).

Later the approach of Refs. [4,5] was extended to the $P_{33}(1232)$ resonance region in a number of works (see, for example, references in Refs. [1,6]), and to the first, second, and third resonance regions in the UIM [1]. The background in the UIM is constructed from the contributions of nucleon exchange in the $s$ and $u$ channels and the $t$ channel $\pi$ exchange with a $\pi NN$ coupling which is pure pseudovector at threshold, transforming with increasing energy into the pseudoscalar coupling via formula (B2). In addition to these contributions, the background of the UIM [1] contains the $t$-channel $\rho$ and $\omega$ exchanges, which are given in Appendix E. The background, constructed in this way, is unitarized for each multipole amplitude according to Ref. [17] in the $K$-matrix approximation:

$$\text{Unitarized}(M_{l\pm},\ E_{l\pm},\ S_{l\pm})_{background}$$
$$=(M_{l\pm},\ E_{l\pm},\ S_{l\pm})_{background}(1+ih_{l\pm}^{\pi N}). \quad (15)$$

This form of the unitarization of the background is equivalent to taking into account on-shell $\pi N$ rescattering in the diagrams contributing to the background. Off-shell rescattering can be found only using models and contains uncertainties connected with the cutoff in corresponding integrals and with the method of taking into account off-shell effects. It is not included into the unitarization procedure [Eq. (15)]. Below the two-pion production threshold, where $h_{l\pm}^{\pi N}=\sin\delta_{l\pm}^{\pi N}\exp(i\delta_{l\pm}^{\pi N})$, unitarization according to Eq. (15) satisfies the Watson theorem for the background contributions into multipole amplitudes.

With increasing energy the contribution of the background of the UIM [1] becomes too large. This is demonstrated in the case of $M_{1+}^{3/2}$ in Fig. 1(d) (dotted curve). In order to compensate these large background contributions, resonance contributions in the UIM of Ref. [1] have been strongly deformed. Continued to the energies $W>2$ GeV, the background of Ref. [1] strongly contradicts experimental data.

Extension of the effective Lagrangian approach above the first resonance region with the minimal set of diagrams (the nucleon exchanges in the $s$ and $u$ channels, and $t$ channel $\pi$, $\rho$, and $\omega$ exchanges) cannot be satisfactory by the following reasons.

(i) Restriction to mesons with lowest masses in the $t$-channel exchanges is justified only at small energies, where $|t|$ is small and, therefore, the propagators $1/(t-m_{mes}^2)$ are determined by the meson masses. However, with increasing energy the range of $t$ is increasing, and additional $t$-channel contributions corresponding to mesons with higher masses should be taken into account.

(ii) With increasing energy, starting with $W=1.3$ GeV, the contributions of inelastic channels into $\pi N$ scattering become important (see, for example, Ref. [18]). This means that diagrams corresponding to the production of other par-

ticles with subsequent rescattering, i.e., $\gamma N \to$ inel. $\to \pi N$, should be taken into account. Therefore in order to extend consistently the effective Lagrangian approach above the first resonance region, it is necessary to take into account a large number of new diagrams.

On the other hand, it is known that with increasing energy Regge-ization of different contributions occurs via multiple gluon exchanges between $t$-channel quarks, and all contributions are reduced to a restricted number of Regge-ized $t$-channel exchanges. This picture, which is known as the Regge-pole model, gives a good description of exclusive reactions above $W = 2.5$ GeV ($E_\gamma = 3$ GeV) at $|t| < 3$ GeV$^2$. In a number of cases the Regge-pole approach gives a good description at smaller energies as well.

For this reason we have modified the unitary isobar model so that it incorporates the results of the effective Lagrangian approach in the first resonance region and the Regge-pole behavior of the amplitudes at high energies. With this aim, the background of the UIM of Ref. [1], which consists of $N$, $\pi$, $\rho$, and $\omega$ contributions and is real, has been modified by including the real parts of the Regge-pole contributions:

$$\text{Back} = [N + \pi + \rho + \omega]_{UIM} \quad \text{at} \quad s < s_0,$$

$$\text{Back} = [N + \pi + \rho + \omega]_{UIM} \frac{1}{1 + (s - s_0)^2} + \text{Re } [\pi + \rho + \omega$$

$$+ b_1 + a_2]_{Regge} \frac{(s - s_0)^2}{1 + (s - s_0)^2} \quad \text{at} \quad s \geqslant s_0. \quad (16)$$

In the resonance energy region, we unitarize Eq. (16) in the K-matrix approximation [Eq. (15)]. From the sum rules which follow from dispersion relations [19–21], it is known that there is an integral duality between imaginary parts of the amplitudes in the resonance energy region and the imaginary parts of the Regge-pole amplitudes, continued into this region. For this reason we do not continue the imaginary parts of the Regge-pole amplitudes below $W = 2$ GeV. Above $W = 2$ GeV the imaginary parts of the amplitudes, which in the resonance energy region are determined by the resonance contributions, will turn into the imaginary parts of the Regge-pole amplitudes.

With the background of the unitary isobar model modified according to Eqs. (16), a good description of all multipole amplitudes with $l \leqslant 3$ has been obtained up to $W = 2$ GeV, taking resonance contributions in the standard Breit-Wigner form presented in Appendix C. The parameter $s_0$ in Eqs. (16) was found from the requirement of the best description of multipole amplitudes and is equal to $s_0 = 1.16$ GeV$^2$. The Regge-pole amplitudes in Eq. (16) were taken from the analysis of high energy photoproduction data made in Ref. [10]. They are presented in Appendix D. The $\pi N$ amplitudes in the unitarization procedure [Eq. (15)] were taken from the GWU(VPI) analysis (the SAID program). The results are presented in Figs. 1(b)–1(d) and 2 by solid curves.

Let us note that for the $P_{33}(1232)$ resonance we have modified the Breit-Wigner parametrization given in Eq. (C1), taking $\Gamma_{total}$ in the form $\Gamma_{total} = \Gamma_\pi (M^2/s)$. This allows to

describe the ratio of the imaginary and real parts of the resonance contributions into $M_{1+}^{3/2}$, $E_{1+}^{3/2}$, and $S_{1+}^{3/2}$ in accordance with the Watson theorem. Let us remind, that the background contributions into these multipoles, unitarized via Eq. (15), satisfy the Watson theorem. In the case of the amplitude $M_{1+}^{3/2}$, which is known with great accuracy, the following modifications are also made.

(a) At $W < 1.3$ GeV the right part of the Eq. (C1) is multiplied by the factor $(W/M)^6$.

(b) At $W > 1.3$ GeV the imaginary and real parts of the resonance contribution are multiplied by the factors $I_{Im}$ and $I_{Re}$,

$$I_{Im} = \frac{(W/1.3)^{2.5}(1.3/M)^6}{1 + 2.4(s - 1.69)^{2.5}}, \quad I_{Re} = \frac{(W/1.3)^{3.5}(1.3/M)^6}{1 + 1.4(s - 1.69)^{2.5}}, \quad (17)$$

where $W$ and $M$ are in units of GeV. These are slight modifications. The obtained resonance contribution into $M_{1+}^{3/2}$ is presented in Figs. 1(c) and 1(d), by dash-dotted curves. It is seen that the sum of this contribution and the unitarized background with $s_0 = 1.16$ GeV$^2$ (dashed curves) describes well the GWU(VPI) data. With the nonmodified bakground (dotted curves), resonance contribution should be strongly deformed in order to describe the GWU(VPI) data.

In order to demonstrate the $Q^2$ evolution of the $P_{33}(1232)$ resonance contribution obtained with the above described modifications, we present in Fig. 4 the imaginary parts of $M_{1+}^{3/2}$ at $Q^2 = 0.9$, 1.8, 2.8, and 4 GeV$^2$ (solid curves). In this figure, Im $M_{1+}^{3/2}$, obtained within DR via a solution of integral equation (8), are also presented (dashed curves). The magnitudes of Im $M_{1+}^{3/2}$ at the resonance position are obtained from the analysis of JLab data [22,23]. It is seen that the amplitudes obtained within the two approaches are in good agreement with each other. In order to compare the shape of the amplitude $M_{1+}^{3/2}$ at $Q^2 \neq 0$ with its shape at $Q^2 = 0$, in Fig. 4, we present the GWU(VPI) data with normalizations corresponding to $Q^2 = 0.9$, 1.8, 2.8, and 4 GeV$^2$. It is seen that the shape of $M_{1+}^{3/2}$ practically is not changed with increasing $Q^2$.

## IV. CONCLUSION

We have obtained a good description of the real parts of all multipole amplitudes with $l \leqslant 3$ up to $W = 1.8$ GeV using fixed-$t$ dispersion relations. In Sec. II A it was shown, that dispersion relations for multipole amplitudes $M_{1+}^{3/2}$, and $E_{1+}^{3/2}$ which correspond to the $P_{33}(1232)$ resonance, can be transformed into singular integral equations. The real and imaginary parts of these multipoles were obtained via solution of these equations and are in good agreement with the GWU(VPI) results.

We have modified the unitary isobar model of Ref. [1] via the incorporation of Regge poles with increasing energy and using the unified Breit-Wigner parametrization of the reso-
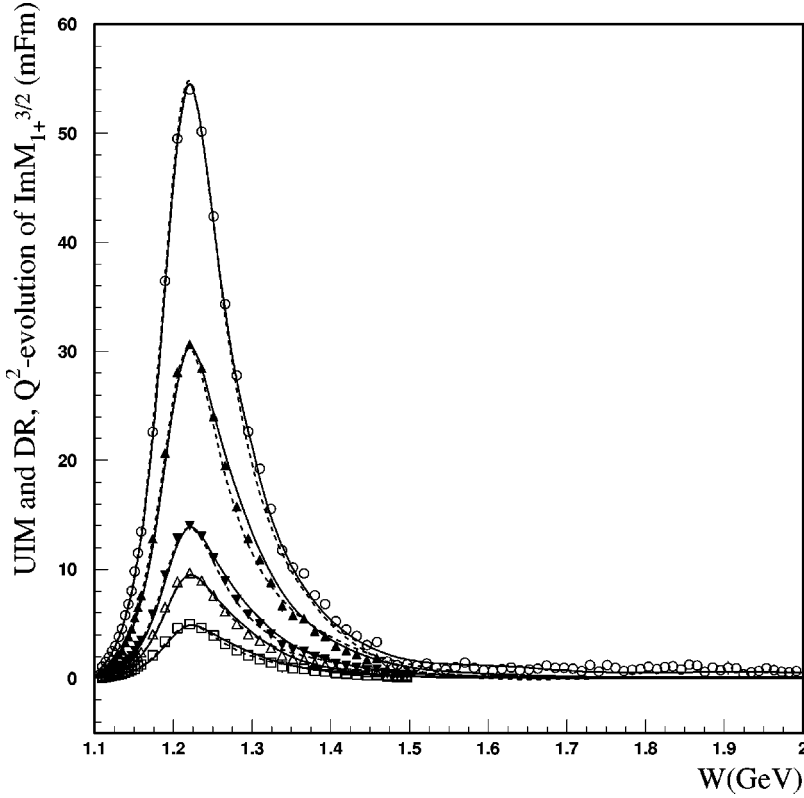
FIG. 4. The imaginary part of $M_{1+}^{3/2}$ obtained within the DR (dashed curves) and UIM (solid curves) at $Q^2 = 0$, 0.9, 1.8, 2.8, and 4 GeV². Data at $Q^2 = 0$ are from GWU(VPI) analysis, and data at other $Q^2$ are the same data with changed normalizations.

nance contributions in the form proposed in Ref. [7]. Within this approach we have obtained a good description of all photoproduction multipoles with $l \leq 3$ up to $W = 2$ GeV.

Both approaches can be continued to $Q^2 \neq 0$, and all formulas of this paper are presented in a form which permits this continuation. Therefore, both approaches can be used for an analysis of data on pion electroproduction on nucleons and for extraction from these data information on the $Q^2$ evolution of $\gamma^* N \to N^*$ form factors. Such data are currently being obtained at the high duty-factor electron accelerator at Jefferson Lab.

### APPENDIX A: RELATIONS BETWEEN INVARIANT AND MULTIPOLE AMPLITUDES

In order to connect invariant and multipole amplitudes it is convenient to introduce the intermediate amplitudes $f_i(s, \cos\theta, Q^2)$:

$$f_1 = [(W - m_N)B_1 - B_5] \frac{[(E_1 + m_N)(E_2 + m_N)]^{1/2}}{8\pi W},$$

$$f_2 = [-(W + m_N)B_1 - B_5] \frac{[(E_1 - m_N)(E_2 - m_N)]^{1/2}}{8\pi W},$$

$$f_3 = \left[ 2B_3 - B_2 + (W + m_N)\left(\frac{B_6}{2} - B_8\right) \right]$$
$$\times \frac{[(E_1 - m_N)(E_2 - m_N)]^{1/2}(E_2 + m)}{8\pi W},$$

$$f_4 = \left[ -(2B_3 - B_2) + (W - m_N)\left(\frac{B_6}{2} - B_8\right) \right]$$
$$\times \frac{[(E_1 + m_N)(E_2 + m_N)]^{1/2}(E_2 - m)}{8\pi W},$$

$$f_5 = \left\{ \left[ Q^2 B_1 + (W - m_N)B_5 + 2W(E_1 - m_N) \right. \right.$$
$$\left. \times \left( B_2 - \frac{W + m_N}{2} B_6 \right) \right] (E_1 + m_N) - X \left[ (2B_3 - B_2) \right.$$
$$\left. \left. + (W + m_N)\left(\frac{B_6}{2} - B_8\right) \right] \right\} \frac{(E_1 - m_N)(E_2 + m_N)}{8\pi W Q^2},$$

$$f_6 = \left\{ -\left[ Q^2 B_1 - (W + m_N) B_5 + 2W(E_1 + m_N) \right.\right.$$
$$\times \left( B_2 + \frac{W - m_N}{2} B_6 \right) \right](E_1 - m_N) + X\left[ (2B_3 - B_2) \right.$$
$$\left.\left. - (W - m_N)\left( \frac{B_6}{2} - B_8 \right) \right]\right\} \frac{(E_1 + m_N)(E_2 - m_N)}{8\pi W Q^2},$$

$$(A1)$$

where

$$X = \frac{\tilde{k}_0}{2}(t - m_\pi^2 + Q^2) - Q^2 \tilde{q}_0,$$ (A2)

$\theta$ is the polar angle of the pion in the c.m.s., and $\tilde{k}_0, \tilde{q}_0, E_1$, and $E_2$ are the energies of the virtual photon, pion, initial, and final nucleons in this system.

The expansions of the intermediate amplitudes over multipole amplitudes $M_{l\pm}(s,Q^2)$, $E_{l\pm}(s,Q^2)$, $S_{l\pm}(s,Q^2)$ have the forms

$$f_1 = \sum \{ (lM_{l+} + E_{l+})P'_{l+1}(\cos\theta)$$
$$+ [(l+1)M_{l-} + E_{l-}]P'_{l-1}(\cos\theta) \},$$

$$f_2 = \sum [(l+1)M_{l+} + lM_{l-}]P'_l(\cos\theta),$$

$$f_3 = \sum [(E_{l+} - M_{l+})P''_{l+1}(\cos\theta)$$
$$+ (E_{l-} + M_{l-})P''_{l-1}(\cos\theta)],$$

$$f_4 = \sum (M_{l+} - E_{l+} - M_{l-} - E_{l-})P''_l(\cos\theta),$$

$$f_5 = \sum [(l+1)S_{l+}P'_{l+1}(\cos\theta) - lS_{l-}P'_{l-1}(\cos\theta)],$$

$$f_6 = \sum [lS_{l-} - (l+1)S_{l+}]P'_l(\cos\theta). \quad (A3)$$

The formulas which relate the amplitudes $f_i(s,\cos\theta,Q^2)$ to the helicity amplitudes and cross section can be found in Ref. [14].

## APPENDIX B: BORN CONTRIBUTION

The residues in the nucleon poles of the invariant amplitudes in Eqs. (3) and (4) are equal to

$$R_1^{(v,s)}(Q^2) = \frac{ge}{2}[F_1^{(v,s)}(Q^2) + 2mF_2^{(v,s)}(Q^2)],$$

$$R_2^{(v,s)}(Q^2) = -\frac{ge}{2}F_1^{(v,s)}(Q^2),$$

$$R_3^{(v,s)}(Q^2) = -\frac{ge}{4}F_1^{(v,s)}(Q^2),$$

$$R_5'^{(v,s)}(Q^2) = \frac{ge}{4}(m_{\pi^2} - Q^2 - t)F_2^{(v,s)}(Q^2),$$

$$R_6^{(v,s)}(Q^2) = geF_2^{(v,s)}(Q^2),$$

$$R_8^{(v,s)}(Q^2) = \frac{ge}{2}F_2^{(v,s)}(Q^2), \quad (B1)$$

where $g^2/4\pi = 14.2$, $e^2/4\pi = 1/137$, and $F_1^{(v,s)}(Q^2)$, $F_2^{(v,s)}(Q^2)$ are the nucleon Pauli form factors. Following Ref. [1], in the UIM the Lagrangian for the $\pi NN$ vertex is taken in the form of mixed pseudovector (PV) and pseudoscalar (PS) couplings,

$$L_{\pi NN} = \frac{\Lambda^2}{\Lambda^2 + q^2}L_{\pi NN}^{PV} + \frac{q^2}{\Lambda^2 + q^2}L_{\pi NN}^{PS}, \quad (B2)$$

where we take $\Lambda^2 = 0.12$ GeV$^2$. This leads to the following additional contributions in the amplitudes $B_1^{(+,0)}(s,t,Q^2)$:

$$B_1^{(+,0)}(s,t,Q^2) = B_1^{(+,0)}(s,t,Q^2) + AF_2^{(v,s)}(Q^2), \quad (B3)$$

where

$$A = \frac{ge}{2m_N}\frac{\Lambda^2}{\Lambda^2 + q^2}. \quad (B4)$$

The nucleon Pauli form factors $F_1^{(v,s)}(Q^2)$ and $F_2^{(v,s)}(Q^2)$ in the above equations we have defined according to the description of the existing data in Refs. [24–26], in the following way:

$$F_1^{(v,s)}(Q^2) = F_{1p}(Q^2) - F_{1n}(Q^2),$$

$$F_2^{(v,s)}(Q^2) = F_{2p}(Q^2) - F_{2n}(Q^2),$$

$$F_{1p}(Q^2) = G_p^m(Q^2)/(1 + 2m_N z), \quad F_{2p}(Q^2) = zF_{1p}(Q^2),$$

$$z = \frac{1.793}{2m_N}\left(1 + \frac{1.2Q^2}{1+1.1Q} + 0.015Q^2 + 0.001Q^8\right),$$

$$G_p^m(Q^2) = 2.793/(1 + 0.35Q + 2.44Q^2 + 0.5Q^3 + 1.04Q^4$$
$$+ 0.34Q^5),$$

$$F_{1n}(Q^2) = \frac{G_n^e(Q^2) + \tau G_n^m(Q^2)}{1 + \tau},$$

$$F_{2n}(Q^2) = \frac{G_n^m(Q^2) - G_n^e(Q^2)}{2m_N(1 + \tau)},$$

$$\tau = Q^2/4m_N^2, \quad G_n^e = \frac{0.5Q^2}{1 + 25Q^4},$$

$$G_n^m(Q^2) = -1.913F_d(Q^2),$$

$$F_d(Q^2) = 1/(1 + 0.71/Q^2). \qquad \text{(B5)}$$

Here $Q^2$ is in units of GeV$^2$. For the pion form factor we take as in Ref. [1] the form

$$F_\pi(Q^2) = F_1^{(v)}(Q^2). \qquad \text{(B6)}$$

## APPENDIX C: BREIT-WIGNER PARAMETRIZATION FOR RESONANCE CONTRIBUTIONS

We use the Breit-Wigner parametrization for the resonance contributions into multipole amplitudes in the form [7,9].

$$\text{Res}_{B-W}(W, Q^2) = c \left( \frac{k}{k_r} \right)^n \left( \frac{q_r}{q} \frac{k_r}{k} \frac{\Gamma_\pi \tilde\Gamma_\gamma}{\eta_\pi \Gamma} \right)^{1/2}$$
$$\times \frac{M\Gamma}{M^2 - W^2 - iM\Gamma_{total}}, \qquad \text{(C1)}$$

where $n=0$ for $M_{l\pm}$, $E_{l\pm}$, $n=1$ for $S_{l\pm}$ and

$$\Gamma_{total} = \Gamma_\pi + \Gamma_{inel}, \qquad \text{(C2)}$$

$$\Gamma_\pi = \eta_\pi \Gamma \left( \frac{q}{q_r} \right)^{2l+1} \left( \frac{X^2 + q_r^2}{X^2 + q^2} \right)^l, \qquad \text{(C3)}$$

$$\tilde\Gamma_\gamma = \left( \frac{k}{k_r} \right)^{2l'+1} \left( \frac{X^2 + k_r^2}{X^2 + k^2} \right)^{l'}, \qquad \text{(C4)}$$

$$\Gamma_{inel} = (1 - \eta_\pi) \Gamma \left( \frac{q_{2\pi}}{q_{2\pi,r}} \right)^{2l+4} \left( \frac{X^2 + q_{2\pi,r}^2}{X^2 + q_{2\pi}^2} \right)^{l+2}. \qquad \text{(C5)}$$

For $M_{l\pm}$, $E_{l+}$, $S_{l+}$, $l'=l$; for $E_{l-}$, $S_{l-}$, $l'=l-2$ if $l \geq 2$; for $S_{1-}$, $l'=1$; $M$ and $\Gamma$ are the masses and widths of the resonances, $\eta_\pi$ are the branching ratios into the $\pi N$ channel, $q_{2\pi}$ is the three-momentum of the $2\pi$ system in the decay Res$\to 2\pi + N$ in the c.m.s., $q_{2\pi,r}$ is the magnitude of this momentum at $W=M$, and $X$ are phenomenological parameters.

For the resonance $S_{11}(1535)$ which has large branching ratio into the $\eta N$ channel, $\Gamma_{total}$ is taken in the form

$$\Gamma_{total} = 0.6\Gamma_\pi + 0.1\Gamma_{inel} + 0.3\Gamma \frac{q_\eta}{q_\eta^r}. \qquad \text{(C6)}$$

Below the thresholds of $2\pi + N$ and $\eta + N$ productions we take, respectively, $q_{2\pi} = 0$ and $q_\eta = 0$.

## APPENDIX D: INVARIANT AMPLITUDES IN THE REGGE REGIME

In Ref. [10] the introduction of Regge-trajectories is made in gauge-invariant form for invariant amplitudes in the following way. Instead of $t$-channel $\pi$ exchange, which is non-gauge-invariant and contributes into $B_3^{(-)}(s,t,Q^2)$, the following combination is used:

$$\bar{u}(p_2) \gamma_5 \{ 2P^\mu B_2^{(-)} + 2q^\mu B_3^{(-)} \} u(p_1), \qquad \text{(D1)}$$

where, in addition to the $\pi$ contribution, the nucleon pole contribution generated by the form factor $F_1^{(v)}(Q^2)$ is taken into account. The nucleon and pion contributions into $B_2^{(-)}$ and $B_3^{(-)}$ are written in the forms

$$B_2^{(-)}(s,t,q^2) = -\frac{ge}{2} F_1^{(v)}(Q^2) \left( \frac{t - m_\pi^2}{s - m^2} - \frac{t - m_\pi^2}{u - m^2} \right) \frac{1}{t - m_\pi^2}, \qquad \text{(D2)}$$

$$B_3^{(-)}(s,t,q^2) = \left[ -\frac{ge}{4} F_1^{(v)}(Q^2) \left( \frac{t - m_\pi^2}{s - m^2} + \frac{t - m_\pi^2}{u - m^2} \right) \right.$$
$$\left. - eg F_\pi(Q^2) \right] \frac{1}{t - m_\pi^2}, \qquad \text{(D3)}$$

and are Regge-ized by the replacement

$$\frac{1}{t - m_\pi^2} \Rightarrow P_{Regge}^\pi \text{ in } B_{2,3}^{(-)} + P_{Regge}^{b_1} \text{ in } B_{2,3}^{(0)}. \quad \text{(D4)}$$

Here $P_{Regge}$ are Regge propagators,

$$P_{Regge}^{\pi,b_1} = \left( \frac{s}{s_0} \right)^{\alpha_\pi(t)} \frac{\pi \alpha'_\pi}{\sin[\pi\alpha_\pi(t)]} \frac{1}{\Gamma[1 + \alpha_\pi(t)]} \frac{\tau + e^{-i\pi\alpha_\pi(t)}}{2}, \qquad \text{(D5)}$$

and it is supposed that $\pi$ and $b_1$ trajectories are degenerate: $\alpha_\pi(t) = \alpha'_\pi(t - m_\pi^2)$, and $\alpha'_\pi = 0.7$ GeV$^{-2}$.

The contributions of the $\rho$ and $\omega$ exchanges in the $t$-channel are gauge invariant and are Regge-ized simply by the following replacements in Eqs. (E1):

$$\frac{1}{t - m_\rho^2} \Rightarrow P_{Regge}^\rho \text{ in } B_i^{(0)} + P_{Regge}^{a_2} \text{ in } B_i^{(-)},$$
$$i = 1,2,3,6, \qquad \text{(D6)}$$

$$\frac{1}{t - m_\omega^2} \Rightarrow P_{Regge}^\omega \text{ in } B_i^{(+)}, \quad i = 1,2,3,6, \quad \text{(D7)}$$

where it is assumed that the $\rho$ and $a_2$ trajectories are degenerate, and

$$P_{Regge}^{\rho,a_2} = \left( \frac{s}{s_0} \right)^{\alpha_\rho(t)-1} \frac{\pi \alpha'_\rho}{\sin[\pi\alpha_\rho(t)]} \frac{1}{\Gamma[\alpha_\rho(t)]} \frac{\tau + e^{-i\pi\alpha_\rho(t)}}{2},$$

$$P_{Regge}^\omega = \left( \frac{s}{s_0} \right)^{\alpha_\omega(t)-1} \frac{\pi \alpha'_\omega}{\sin[\pi\alpha_\omega(t)]} \frac{1}{\Gamma[\alpha_\omega(t)]} \frac{\tau + e^{-i\pi\alpha_\omega(t)}}{2}, \qquad \text{(D8)}$$

$\alpha_\rho(t) = 0.55 + \alpha'_\rho t$, $\alpha'_\rho = 0.8$ GeV$^{-2}$, $\alpha_\omega(t) = 0.44 + \alpha'_\omega t$, $\alpha'_\omega = 0.9$ GeV$^{-2}$. In Eqs. (D5) and (D8), $\tau$ is the signature of the trajectory:

$$\tau_\pi = \tau_{a_2} = 1, \quad \tau_\rho = \tau_\omega = \tau_{b_1} = -1. \tag{D9}$$

## APPENDIX E: $\rho$ AND $\omega$ CONTRIBUTIONS

The $\rho$ and $\omega$ exchanges in the $t$ - channel contribute to the following amplitudes:

$$B_1^{(0)} = \frac{e\lambda_\rho}{m_\pi} \left[ 2m_N g_{\rho1} + t \frac{g_{\rho2}}{2m_N} \right] \frac{1}{t - m_\rho^2},$$

$$B_2^{(0)} = \frac{e\lambda_\rho}{m_\pi} \frac{g_{\rho2}}{4m_N} (Q^2 + m_\pi^2 - t) \frac{1}{t - m_\rho^2},$$

$$B_3^{(0)} = \frac{e\lambda_\rho}{m_\pi} \frac{g_{\rho2}}{8m_N} (u - s) \frac{1}{t - m_\rho^2}, \quad B_6^{(0)} = 2\frac{e\lambda_\rho}{m_\pi} g_{\rho1} \frac{1}{t - m_\rho^2},$$

$$B_1^{(+)} = \frac{e\lambda_\omega}{m_\pi} \left[ 2m_N g_{\omega1} + t \frac{g_{\omega2}}{2m_N} \right] \frac{1}{t - m_\omega^2},$$

$$B_2^{(+)} = \frac{e\lambda_\omega}{m_\pi} \frac{g_{\omega2}}{4m_N} (Q^2 + m_\pi^2 - t) \frac{1}{t - m_\omega^2},$$

$$B_3^{(+)} = \frac{e\lambda_\omega}{m_\pi} \frac{g_{\omega2}}{8m_N} (u - s) \frac{1}{t - m_\omega^2}, \quad B_6^{(+)} = 2\frac{e\lambda_\omega}{m_\pi} g_{\omega1} \frac{1}{t - m_\omega^2}. \tag{E1}$$

These amplitudes are obtained using vertices $\gamma\rho\pi$, $\gamma\omega\pi$, $\rho NN$, and $\omega NN$ defined in the form presented in Ref. [1]. In the UIM, the off-shell behavior of $g_{Vi}$ is described by: $g_{Vi} = \tilde{g}_{Vi} \Lambda_V^2 / (\Lambda_V^2 - t)$. The coupling constants are taken from Ref. [1], and are equal to

$$\lambda_\omega = 0.314, \quad \tilde{g}_{\omega1} = 21, \quad \tilde{g}_{\omega2} = -12, \quad \Lambda_\omega = 1.2,$$

$$\lambda_\rho = 0.103, \quad \tilde{g}_{\rho1} = 2, \quad \tilde{g}_{\rho2} = 13, \quad \Lambda_\rho = 1.5. \tag{E2}$$

In the Regge-pole analysis of high energy photoproduction data in Ref. [10] the coupling constants are

$$g_{\omega1}^{Regge} = 13.9, \quad g_{\omega2}^{Regge} = 0, \quad g_{\rho1}^{Regge} = 3.47, \quad g_{\rho2}^{Regge} = 13. \tag{E3}$$

[1] D. Drechsel, O. Hanstein, S.S. Kamalov, and L. Tiator, Nucl. Phys. **A645**, 145 (1999).

[2] R.A. Arndt, I.I. Strakovsky, and R.L. Workman, Phys. Rev. C **53**, 430 (1996).

[3] R.A. Arndt, W.J. Briscoe, I.I. Strakovsky, and R.L. Workman, nucl-th/0205067.

[4] S. Weinberg, Phys. Rev. Lett. **18**, 188 (1967); Phys. Rev. **166**, 1568 (1968).

[5] R.D. Peccei, Phys. Rev. **181**, 1902 (1969).

[6] R.M. Davidson, N.C. Mukhopadhyay, and R.S. Witman, Phys. Rev. D **43**, 71 (1991).

[7] R.L. Walker, Phys. Rev. **182**, 1729 (1969).

[8] K.M. Watson, Phys. Rev. **95**, 228 (1954).

[9] R.C.E. Devenish and D.H. Lyth, Phys. Rev. D **5**, 47 (1972).

[10] M. Gidal, J.-M. Laget, and M. Vanderhaegen, Nucl. Phys. **A627**, 645 (1997); Phys. Lett. B **400**, 6 (1997).

[11] R.A. Arndt, I.I. Strakovsky, R.L. Workman, and M.M. Pavan, Phys. Rev. C **52**, 2120 (1995).

[12] D. Schwela, H. Rolnik, R. Weizel, and W. Korth, Z. Phys. **202**, 452 (1967).

[13] D. Schwela and R. Weizel, Z. Phys. **221**, 71 (1969).

[14] I.G. Aznauryan, Phys. Rev. D **57**, 2727 (1998).

[15] R.C.E. Devenish and D.H. Lyth, Nucl. Phys. **B93**, 109 (1975).

[16] R.L. Crawford, Nucl. Phys. **B97**, 125 (1975).

[17] S.S. Kamalov *et al.*, Phys. Rev. C **64**, 032201(R) (2001).

[18] R.A. Arndt *et al.*, Phys. Rev. D **43**, 2131 (1991).

[19] A.A. Logunov, L.D. Soloviev, and A.N. Tavkhelidze, Phys. Lett. B **24**, 181 (1967).

[20] I.G. Aznauryan and L.D. Soloviev, Phys. Lett. **28B**, 597 (1969).

[21] I.G. Aznauryan and L.D. Soloviev, Yad. Fiz. **11**, 870 (1970).

[22] V.V. Frolov *et al.*, Phys. Rev. Lett. **82**, 45 (1999).

[23] K. Joo *et al.*, Phys. Rev. Lett. **88**, 122001 (2002).

[24] M.K. Jones *et al.*, Phys. Rev. Lett. **84**, 1398 (2000).

[25] Kees de Jager, JLAB preprint JLAB-PHY-00-01.

[26] P. Bosted, Phys. Rev. C **51**, 409 (1995).